engineering proceedings

MDPI

Proceeding Paper

Vibroacoustic Optimization of the Airframe Using Energy Harvesting Resonators: An Experimental and Numerical Approach †

Florian Mock *, Lukas Kettenhofen, Daniel Alboldt and Kai-Uwe Schröder

Institute of Structural Mechanics and Lightweight Design, RWTH Aachen University, Wüllnerstraße 7, 52066 Aachen, Germany; lukas.kettenhofen@sla.rwth-aachen.de (L.K.); daniel.alboldt@sla.rwth-aachen.de (D.A.); kai-uwe.schroeder@sla.rwth-aachen.de (K.-U.S.)

* Correspondence: florian.mock@sla.rwth-aachen.de

† Presented at the 15th EASN International Conference, Madrid, Spain, 14–17 October 2025.

Abstract

The open fan as a highly efficient propulsion concept is a promising approach to reduce climate-damaging emissions in aviation. However, the increased vibroacoustic emissions of the fan resulting from the open design lead to elevated cabin noise. Energy harvesting resonators can be used to leverage the piezoelectric effect and to attenuate structural vibrations caused by the acoustic loading simultaneously. To evaluate the potential of a specific configuration of energy harvesting resonators, an investigation of the dynamic interaction between the airframe and the resonators is necessary. Therefore, the eigenmodes and eigenfrequencies of a representative stiffened plate are determined experimentally using modal analysis via laser scanning vibrometry. A finite element model of the stiffened plate with the resonator idealized as a mass–spring element is implemented. The stiffness of this simplified resonator model is calibrated by correlating simulated with experimental results following a model updating approach. Finally, an optimization framework designed to determine the optimal quantity and placement of resonators using the experimentally validated model and representative loads is implemented to maximize both vibroacoustic attenuation and energy harvesting efficiency. The resulting framework serves as a generalized optimization tool capable of systematically optimizing the resonator configuration based on airframe geometry and specified vibroacoustic loading scenarios.

Keywords: modal analysis; model updating; vibration control; vibroacoustic optimization

Check for updates

Academic Editors: Spiros Pantelakis, Andreas Strohmayer and Gustavo Alonso

Published: 15 May 2026

Corrected: 17 August 2026

Copyright: © 2026 by the authors. Licensee MDPI, Basel, Switzerland. This article is an open access article distributed under the terms and conditions of the Creative Commons Attribution (CC BY) license.

1. Introduction

A primary objective of modern aviation research is the reduction in climate-damaging emissions from aircraft. The aviation industry proclaims the aim of achieving net CO_2 emissions of zero by the year 2050 [1]. To reduce fuel consumption and thus CO_2 emissions, the aircraft mass is minimized through the use of thin-walled lightweight structures, which, however, exhibit high vibroacoustic excitability. Another approach to reduce CO_2 emissions involves the utilization of alternative propulsion concepts. For instance, propeller propulsion systems in an open-fan design are highly efficient but also result in significant vibroacoustic loads on the airframe. This leads, particularly in combination with thin-walled structures, to vibrations that can propagate through the wing structure or the surrounding air into the fuselage structure contributing to increased cabin noise

levels. To enhance the acceptance of new propulsion technologies, it is essential that passenger comfort remains unaffected. Therefore, research is being conducted on minimizing vibrations due to vibroacoustic loads within the fuselage structure. A positive effect of resonators on the vibroacoustic behavior of aircraft fuselage structures has already been shown in [2]. In the research project EMPreSs, vibration reduction is being investigated through the application of energy harvesting resonators on the airframe, Figure 1. These resonators are intended to minimize structural vibrations in an adjustable frequency range while simultaneously harvesting electrical energy from the vibrations via the piezoelectric effect. The applicability of differently designed energy harvesting resonators for vibration reduction has been demonstrated in [3], but there is no optimization framework available to determine the optimal arrangement of the resonators.



Figure 1. Mounting brackets for energy harvesting resonators attached to a stiffened plate as a model for the airframe.

In this study, the dynamic properties of the resonators will be determined experimentally, and a modeling approach will be developed to facilitate their simulation within numerical models. As a test object, a flat, stiffened plate approximating a fuselage structure in a stringer–frame construction is being investigated, Figure 1. Two stringers and frames are adhesively bonded to the plate forming an inner skin section, which is completely surrounded by stiffeners. Using laser scanning vibrometry, the eigenmodes and eigenfrequencies of the surrounded section, both with and without a resonator, are determined within a frequency range of 0 Hz to 800 Hz. The resulting frequency spectra show significantly smaller amplitudes of the eigenmodes for the plate with a resonator from approximately 130 Hz up to the upper limit of the examined frequency range compared to the plate without a resonator. The experimental results are subsequently compared with simulation results obtained from a frequency analysis of the finite element (FE) model of the plate. Thereafter, the stiffness parameters of the adhesives and the resonator in the FE models are adjusted until the deviation in eigenfrequencies between the experimental and simulated results, averaged over the examined frequency range, is minimized. A minimal average frequency deviation of 0.62 % is achieved. Finally, the FE model of the stiffened plate is utilized to optimize the number and placement of resonators numerically. In order to minimize the structural vibrations, the resonators are moved until the sum of the displacements calculated in a steady-state analysis at every node of the inner plate section reaches its minimum. The optimization process is performed for different quantities of resonators ranging from one to four. With higher numbers of resonators, a higher reduction in structural vibrations is observed, whereas the difference in vibration reduction between three and four resonators is already marginal. The lowest vibration level for all numbers of resonators is achieved when placing all resonators in the middle of the inner plate section. For resonator numbers greater than one, this leads to a very close placement of the resonators.

https://doi.org/10.3390/engproc2026133150

2. Materials and Methods

The stiffened plate is constructed from individual components made of the aluminum alloy AlMg3. A technical drawing with the dimensions of the plate is shown in Figure 2a. The thickness of the ground plate is 1.5 mm. While the stringers are directly bonded to the plate, the frames are attached using clips with a distance of 30 mm from the plate. The aviation-approved epoxy adhesive *Scotch-Weld 9323 B/A* from *3M, St. Paul, MN, USA* is utilized to bond the components. To ensure optimal adhesion, the bonding surfaces are initially cleaned with a solvent and subsequently roughened with sandpaper and a curing period of 15 days at room temperature is observed. The total weight of the stiffened plate amounts to 6.95 kg. The resonator weighs 42.3 g including its mounting bracket, which is glued to the stiffened plate as shown in Figure 1.

The plastic mounting bracket is positioned on the rear side of the stiffened plate at the center of the inner skin section to facilitate an even distribution of measurement points on the front side. Following examples from [4,5], the stiffened plate is suspended by stiff ropes during the experiments for the investigation of their dynamic properties, Figure 2b. This method of support was chosen to resemble free boundary conditions of the plate after excitation. Consequently, the recorded vibrations correspond to the eigenfrequencies of the unaffected structure. Additionally, this approach aims to decouple the plates from the suspension and minimize rigid-body vibrations of the plate along the vertical axis, thereby avoiding excitation of the overall system comprising both the plate and suspension.



(**a**) (**b**) (**c**)

Figure 2. Experimental setup for the modal analysis of the stiffened plate. (**a**) Technical drawing of the stiffened plate. (**b**) LDSVs and suspended plate. (**c**) Modal hammer on the rear side, R: resonator position.

For the investigation of the plates, the *PSV QTec-3D*, a 3D laser vibrometer consisting of three laser Doppler scanning vibrometers (LDSVs) from *Polytec, Waldbronn, Germany*, is employed. To achieve optimal measurement results, the LDSVs are arranged in an equilateral triangle as recommended by the manufacturer, Figure 2b. In the experimental setup utilized, measurements are conducted at an angle from the side to allow for a comprehensive assessment of the skin section despite the overhanging edge caused by the Z-profile of one stringer. The distance between the measurement devices and the suspended plates is approximately 2.8 m.

To determine the dynamic properties of the stiffened plates, a shock excitation is applied by the electronic modal hammer *SAM 1* from *NV-Tech, Steinheim, Germany*, Figure 2c. The hammer impulse simultaneously excites many eigenfrequencies across a broad frequency spectrum [6]. Following the excitation, there is no further influence on the plate

from the hammer, allowing for free vibration of the plate. To ensure unobstructed visibility for the LDSVs on the measurement objects, excitation occurs on the rear side of the plate. A steel hammer tip is employed to achieve a short contact time, thereby approximating an ideal impulse.

The model for the simulated modal analysis of the stiffened plate is created in *Abaqus, 2020*. The individual components, which can be regarded as thin-walled, are modeled with shell elements and the isotropic material behavior of AlMg3 is assigned. After assembling the components, the assembly is meshed using a mesh size of 5 mm. The adhesive surfaces are simulated using the *Abaqus* function *cohesive behavior* that allows for the specification of the required stress for relative displacement of the connected components in both normal and shear directions by defining three values k_{nn}, k_{ss} and k_{tt}. The resonator is modeled as a point mass with a mass of 42.3 g, positioned in the center of the inner skin section at a distance of 5 mm from the plate surface, and is connected to the plate by six spring elements. Only the translational degree of freedom perpendicular to the plate plane is assigned a realistic spring stiffness, while the other five degrees of freedom are constrained by very high spring stiffnesses.

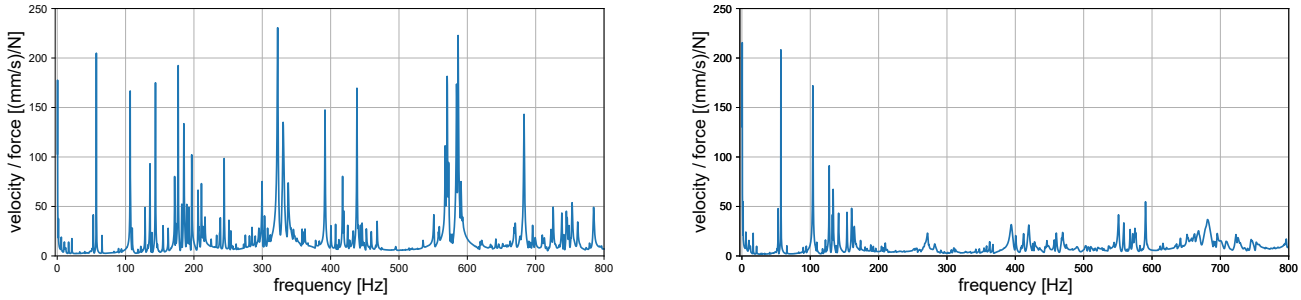
The eigenmodes of the stiffened plate are determined through a frequency analysis employing the *Lanczos* solution method. In accordance with the experiments, eigenmodes up to 800 Hz are calculated. Following a model updating approach [7], efforts are made to align the eigenmodes computed in simulations as closely as possible with experimental results. The outcomes of the simulated modal analysis on the adjusted FE models are evaluated by comparing the eigenmodes and determining deviations in natural frequencies compared to experimental data across the entire frequency spectrum. For the resonator, mechanical properties of the spring elements and for the adhesive layer, the stiffness parameters k_{nn}, k_{ss} and k_{tt} are iteratively adjusted until further iterations do not yield smaller discrepancies between simulation results and measurements. In this manner, an experimentally validated model of the stiffened plate with the resonator is created, which can subsequently be utilized for a numerical optimization of the resonator's position on the plate.

The objective of the optimization is to determine the optimal distribution for one or more resonators in order to minimize the vibrations of the plate and consequently cabin noise for a given excitation. That is why the sum of absolute displacements at all nodes within the inner skin section, calculated in a steady-state analysis, is selected as the objective function for optimization. The *SLSQP* solver, a gradient-based optimization algorithm from the *scipy.optimize* library in Python (version 3.12), is employed for this purpose. The algorithm iteratively modifies the positions of the resonators in both x and y directions by 1 mm to calculate an approximate value for the derivative of the objective function at the current resonator positions. Based on this information, new resonator positions are determined until convergence is achieved. However, since the optimization problem is non-convex, it may converge to local optima that are far from the global optimum. To address this issue, eight optimizations with different initial positions of the resonators are initiated in parallel for each number of resonators. One initial position is always a uniform distribution across the inner plate segment, while the remaining initial positions are randomly selected using *Latin Hypercubes*. An external excitation with a frequency of between 149.5 Hz and 150.5 Hz is assumed, based on a typical value for the first blade pass frequency of a propeller propulsion. The excitation load is applied as a uniformly distributed pressure with an amplitude of 20 Pa, which corresponds to a sound pressure level of 120 dB. To draw conclusions about a trend in the effectiveness of vibration minimization, the optimization is conducted for 1, 2, 3 and 4 resonators.

3. Results

3.1. Experimental Results

The experimental investigation of the stiffened plate yields frequency spectra both without and with the attached resonator, Figure 3. In these frequency spectra, the velocity perpendicular to the plate surface related to the excitation force is plotted against the frequency over a range of 0 Hz to 800 Hz. Both frequency spectra exhibit a peak at a frequency of 0.5 Hz, which describes the rigid-body motion of the suspended plate. This motion is dependent solely on the support conditions and should not be considered as an eigenmode of the stiffened plate; therefore, it does not contribute to further analyses.

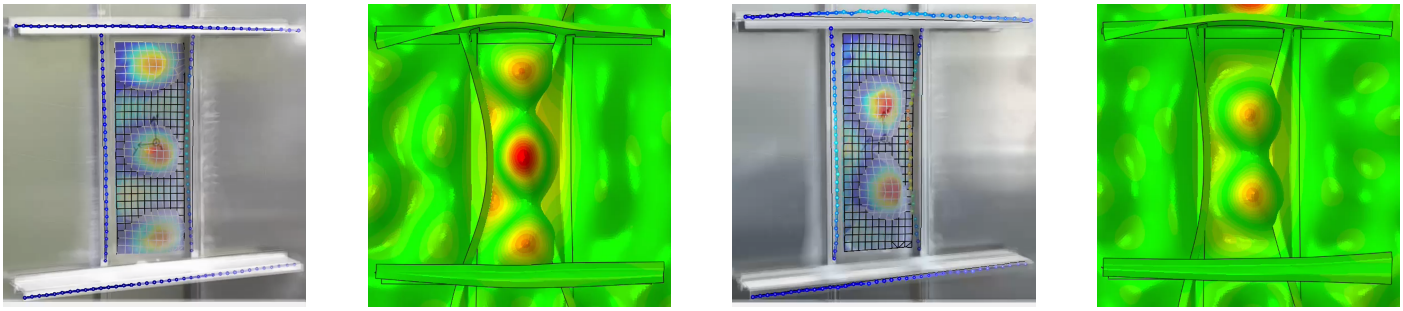


(**a**) (**b**)

Figure 3. Frequency spectra of stiffened plate from 0 Hz to 800 Hz. (**a**) Stiffened plate without resonator. (**b**) Stiffened plate with resonator.

The remaining peaks indicate the frequencies of the eigenmodes of the stiffened plate. The shape of these eigenmodes becomes evident through the evaluation of experimental data. A comparison of the frequency spectra clearly shows that amplitudes with the resonator are significantly smaller than those without it starting from approximately 130 Hz. In certain frequency ranges, amplitudes are reduced to about one-tenth by applying the resonator. The effect is most pronounced in the range between 320 Hz and 350 Hz, where the frequency spectrum of the bonded plate without a resonator displays three medium-to-high peaks. The corresponding eigenmodes reveal three half-waves across the inner skin section. Thus, in the middle of this skin section, where the resonator is located, there exists an antinode that excites the resonator.

A visual comparison of modes further demonstrates that many mode shapes change significantly due to the presence of the resonator. Two unique eigenmodes for each frequency spectrum are illustrated in Figure 4a,c. It can be concluded that a single resonator has a significant impact on the dynamic behavior of the stiffened plate and reduces the vibration amplitudes in this experimental setup over a wide frequency range.



(**a**) (**b**) (**c**) (**d**)

Figure 4. Examples of eigenmodes of the stiffened plate found in the experiments and the simulation. (**a**) Experiment, without a resonator at 586 Hz. (**b**) Simulation, without a resonator at 589 Hz. (**c**) Experiment, with a resonator at 590 Hz. (**d**) Simulation, with a resonator at 594 Hz.

3.2. Simulation Results

Using the model of the stiffened plate described in the Materials and Methods Section, a modal analysis shows that for nearly all eigenmodes identified in the experiments, a corresponding eigenmode is simulated. Examples of the correlation between experiment and simulation are presented in Figure 4. To achieve an accurate representation of reality, the stiffness parameters of the adhesive connections and the spring of the modeled resonator are iteratively adjusted according to the principle of model updating [7]. The relative deviation between experiment and simulation is assessed across the investigated frequency range from 0 Hz to 800 Hz. The smallest deviations are found for the stiffness values of the adhesive, k_{nn} = 5000 N/mm^3 and $k_{ss} = k_{tt}$ = 4250 N/mm^3, and for the spring stiffness of the resonator k_{res} = 750 N/mm. This results in an average frequency deviation of 1.23% for the stiffened plate without a resonator and 0.62% for the plate with a resonator.

Furthermore, the influence of the resonator on the shape of eigenmodes is also well represented by the simulation. Numerous examples demonstrate that changes in vibrations observed in experimental results are consistently calculated by the simulation. Overall, after model updating, a validated simulation model for the stiffened plate with a resonator emerges, which can compute the structural response of the plate to external excitation. This model can subsequently be used to investigate and optimize the effectiveness of vibration reduction for various arrangements and numbers of resonators.

3.3. Optimization Results

The results of the optimization initially reveal a clear trend that the use of more resonators leads to lower sums of displacements and, consequently, reduced amplitudes of vibrations. In Figure 5, the best results from the eight optimizations for each number of resonators are examined while the numerical values are summarized in Table 1. However, the curve representing the sum of displacements appears to be approaching a minimum with four resonators, suggesting that adding further resonators may not yield additional reductions in the sum of displacements. Conversely, the mass added by the resonators increases linearly with the number of resonators.

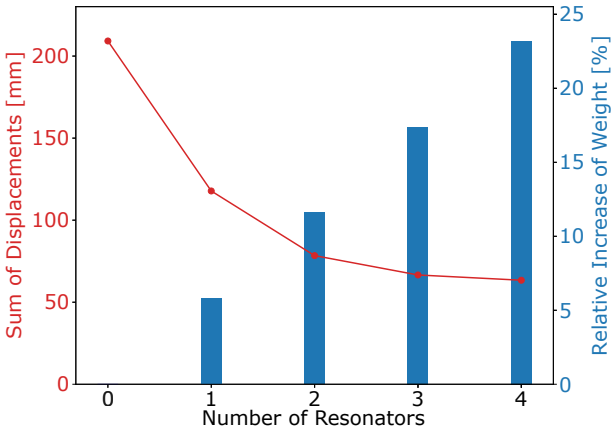


Figure 5. Optimization results: Sum of displacements in red and additional relative mass in blue over number of resonators.

The result of the optimization for one resonator shows that the position converges to a point near the center of the inner skin section to minimize the sum of displacements, Figure 6a. This behavior is also observed for multiple resonators. Among the best optimization results, several resonators are arranged close to the center of the plate and only a few millimeters apart from each other. The close positioning of resonators for the optimal

results is illustrated in Figure 6b for the case of two resonators, where points in the same color represent the positions of the two resonators from one optimization.

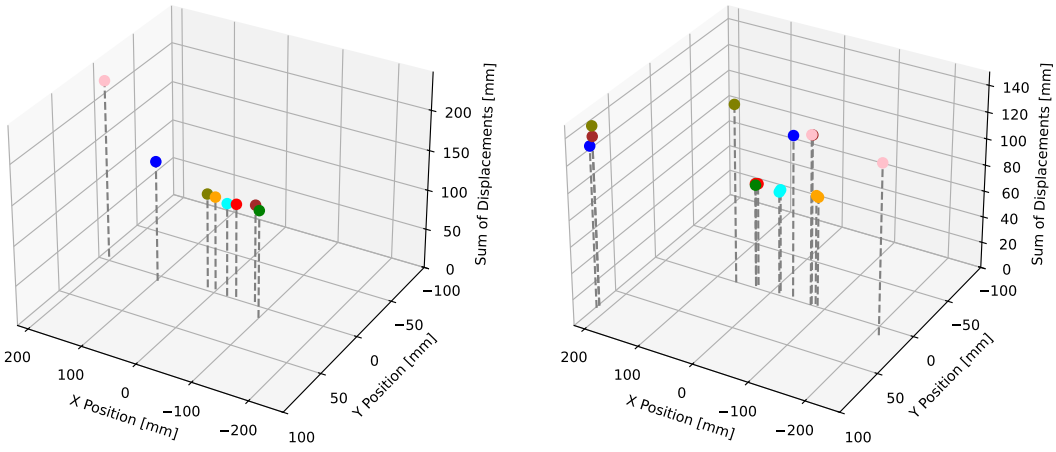


Figure 6. Optimization results: Positions (dashed lines on X-Y-surface) and sum of displacements. (**a**) One resonator. (**b**) Two resonators.

Table 1. Numerical optimization results.

Number of Resonators	Sum of Displacements [mm]	x Positions [mm]	y Positions [mm]
0	209.2	—	—
1	117.8	−23	−1
2	78.4	32; 30	−4; −2
3	66.6	4; −1; 3	−7; −12; −8
4	63.4	−5; −6; −7; −9	−20; −16; −17; −17

4. Discussion

The comparison of the frequency spectra from the experimental results reveals particularly significant effects of the resonator between 320 and 350 Hz. This observation is highlighted by a logarithmic plotting of the amplitudes, Figure 7. In the frequency range of approximately 290 Hz to 350 Hz, the largest difference in amplitudes between the stiffened plate without and with the resonator can be observed, allowing this frequency range to be interpreted as a stop band. The pronounced minimization of vibration amplitude within this frequency range aligns well with previous investigations of a former resonator design, which exhibited a stop band between 200 Hz and 400 Hz [3].

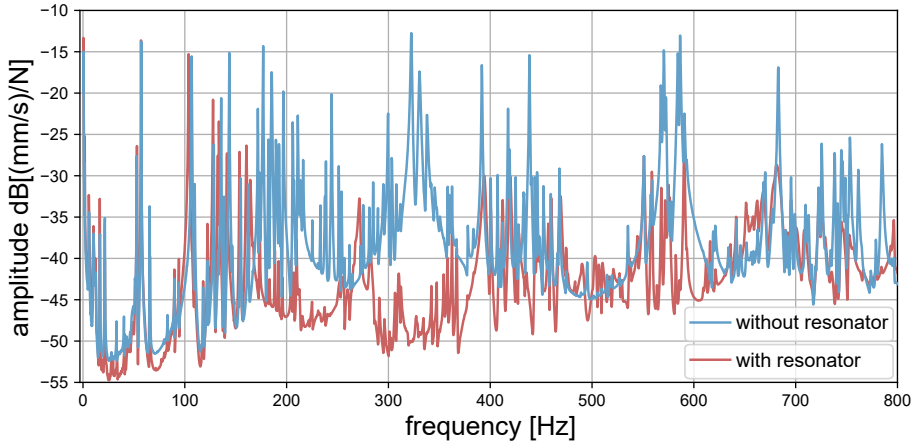


Figure 7. Frequency spectrum without and with resonator in logarithmic representation.

As the resonator is located on the rear side of the plate outside the view of the LDSVs, it is not possible to directly measure its dynamic properties. In future experiments, positioning the resonator on the front side will allow for investigation into whether the resonator is excited and if these vibrations correspond with the frequencies within the stop band. However, the identified stop band between 290 Hz to 350 Hz cannot account for the reduction in amplitudes at higher frequencies. A possible explanation could be the additional mass of the resonator in the middle of the inner section, which fundamentally influences its dynamic properties. In addition, the excitation occurs at a slightly offset point and close to the resonator, which may also affect the vibrations induced in the plate.

In the optimization, it is assumed that lower displacements lead to reduced sound levels. However, the actual acoustics of a stiffened plate are more complex. In future work, the use of an objective function reflecting reality better would be beneficial. Furthermore, it would be interesting to investigate the influence of different excitation frequencies and broader frequency ranges on the optimization results.

5. Conclusions

In this study, the influence of an energy harvesting resonator on the dynamic properties of a stiffened plate is experimentally investigated. The results demonstrate that the resonator significantly reduces vibration amplitudes in a frequency range from approximately 130 Hz to 800 Hz. A stop band is identified between 290 Hz and 350 Hz, where the resonator has the most pronounced effect on amplitude reduction. Based on the experimental results, an FE model of the stiffened plate with the resonator is adjusted until a close match is achieved between the eigenmodes determined in experiments and simulations. This validated model is then used to optimize the positions of one or more resonators on the plate regarding minimized vibrations. After an optimization with four resonators, the displacements caused by the vibrations at an external excitation with a frequency of 150 Hz are reduced by nearly 70 % compared to the plate without resonators.

Author Contributions: Conceptualization, F.M., L.K. and K.-U.S.; methodology, F.M. and L.K.; software, F.M.; validation, F.M. and L.K.; formal analysis, F.M. and L.K.; investigation, F.M. and L.K.; resources, K.-U.S.; data curation, F.M. and D.A.; writing—original draft preparation, F.M.; writing—review and editing, L.K. and K.-U.S.; visualization, F.M.; supervision, K.-U.S.; project administration, D.A.; funding acquisition, K.-U.S. All authors have read and agreed to the published version of the manuscript.

Funding: The work in this paper was funded by the Federal Ministry for Economic Affairs and Climate Action (Bundesministerium für Wirtschaft und Klimaschutz) of the German government under the funding code 20E2212A.

Institutional Review Board Statement: Not applicable.

Informed Consent Statement: Not applicable.

Data Availability Statement: Data are contained within the article.

Conflicts of Interest: The authors declare no conflicts of interest.

References

1. Air Transport Action Group. Waypoint 2050: Balancing Growth in Aviation with Climate Goals. 2021. Available online: https://aviationbenefits.org/media/167417/w2050_v2021_27sept_full.pdf (accessed on 30 October 2025).
2. Droz, C.; Robin, O.; Ichchou, M.; Atalla, N. Improving sound transmission loss at ring frequency of a curved panel using tunable 3D-printed small-scale resonators. *J. Acoust. Soc. Am.* **2019**, *145*, EL72–EL78. [CrossRef] [PubMed]
3. Mildenberger, J.; Esposito, D.; Holzmann, H.; Atzrodt, H. On the use of ferroelectret metamaterials towards noise mitigation and self-powered sensing in aviation. *Smart Mater. Struct.* **2025**, *34*, 055013. [CrossRef]

4. Dourado, M.D.M.; de Meireles, J.F.B. A Simplified Finite Element Riveted Lap Joint Model in Structural Dynamic Analysis. *Adv. Mater. Res.* **2014**, *10*, 185–191. [CrossRef]
5. Bograd, S.; Schmidt, A.; Gaul, L. Modeling of damping in bolted structures. In *Proceedings of the VDI-Wissensforum: Schwingungsdämpfung (VDI Reports 2003), Wiesloch, Germany, 16–17 October 2007*; VDI-Wissensforum: Düsseldorf, Germany, 2007; pp. 97–110.
6. Kuttner, T.; Rohnen, A. *Praxis der Schwingungsmessung: Messtechnik und Schwingungsanalyse mit MATLAB®*; Springer Vieweg: Wiesbaden, Germany, 2019.
7. Maia, N.M.M.; Silva, J.M.M. *Theoretical and Experimental Modal Analysis*; Research Studies Press: Baldock, UK, 1997.

Disclaimer/Publisher's Note: The statements, opinions and data contained in all publications are solely those of the individual author(s) and contributor(s) and not of MDPI and/or the editor(s). MDPI and/or the editor(s) disclaim responsibility for any injury to people or property resulting from any ideas, methods, instructions or products referred to in the content.